The impact of perturbations to ocean-model parameters on climate and climate change in a coupled model

**Chris M. Brierley · Matthew Collins ·
Alan J. Thorpe**

Abstract Assessments of the impacts of uncertainties in parameters on mean climate and climate change in complex climate models have, to date, largely focussed on perturbations to parameters in the atmosphere component of the model. Here we expand on a previously published study which found the global impacts of perturbed ocean parameters on the rate of transient climate change to be small compared to perturbed atmosphere parameters. By separating the climate-change-induced ocean vertical heat transport in each perturbed member into components associated with the resolved flow and each parameterisation scheme, we show that variations in global mean heat uptake in different perturbed versions are an order of magnitude smaller than the average heat uptake. The lack of impact of the perturbations is attributed to (1) the relatively small impact of the perturbation on the direct vertical heat transport associated with the perturbed process and (2) a compensation between those direct changes and indirect changes in heat transport from other processes. Interactions between processes and changes appear to combine in complex ways to limit ensemble spread and uncertainty in the rate of warming. We also investigate regional impacts of the perturbations that may be important for climate change predictions. We find variations across the ensemble that are significant when measured against natural variability. In terms of the experimental set-up used here (models without flux adjustments) we conclude that perturbed physics ensembles with ocean parameter perturbations are an important component of any probabilistic estimate of future climate change, despite the low spread in global mean quantities. Hence, careful consideration should be given to assessing uncertainty in ocean processes in future probabilistic assessments of regional climate change.

Keywords Climate · Ocean · Parameter · Uncertainty · Ensemble prediction

C. M. Brierley
Department of Meteorology,
University of Reading, Reading, UK

M. Collins
Hadley Centre, Met. Office, Exeter, UK

A. J. Thorpe
Natural Environment Research Council, Swindon, UK

C. M. Brierley (✉)
Department of Geology and Geophysics, Yale University,
210 Whitney Avenue, New Haven, CT, USA
e-mail: Christopher.Brierley@yale.edu

1 Introduction

There is considerable uncertainty in projections of both global and regional climate change from different climate models, which complicates the formulation of mitigation approaches and local adaptation policies (Meehl et al. 2007). This uncertainty comes from a variety of sources: uncertainty in the future climate forcings, uncertainty in the initial climate state (that is from natural variability) and uncertainties related to the numerical model used to make the projections. This latter source of uncertainty may be further divided into uncertainty relating to the model design (which we loosely term structural uncertainty) and uncertainty relating to the value of parameters contained in the physics parameterisations (parameter uncertainty).

Climate models have a finite resolution and cannot explicitly resolve all the important dynamical and physical

processes, so parameterisation schemes are required to incorporate unresolved processes. Climate models will always require parameterisation schemes, as they will always have a finite resolution. Thus, there will also always be some uncertainty associated with the parameters involved in these parameterisations. Collins et al. (2007, henceforth C&07) presented the global mean results from the first ensemble created to investigate the effects of parameter uncertainty in the ocean component of a fully 3-dimensional complex atmosphere-ocean general circulation model. They were just able to detect variations in the global rate of transient warming caused by perturbations made to the ocean parameters. The impacts were less than anticipated and were caused in part by changes in atmospheric properties.

The purpose of this article is twofold; to investigate the reason for the small global mean impacts and to look for local impacts that might be important for regional climate predictions. As a precursor to determining the reason for the results of C&07, the perturbed physics ensemble will be described in additional detail and their global results will be put in the context of other work. The mechanisms by which the physics perturbations influence (or not) the ocean heat balance and uptake will be investigated to help explain the relatively small global impacts seen by C&07. The final goal of much of the work looking at perturbed parameter ensembles is to produce a probabilistic climate forecasting system, and the final section of this work investigates the regional impacts of ocean parameter uncertainty to determine whether perturbed ocean physics needs to be included in these systems.

2 Creation and description of the perturbed ocean physics ensemble

The preliminary step in creating the perturbed physics ensemble was to determine the desired parameters and their ranges, which was done in consultation with experts in ocean modelling. This work uses the third version of the Hadley Centre's coupled atmosphere-ocean general circulation model (HadCM3, Gordon et al. 2000). The parameters chosen were expected to be specific to HadCM3, so the experts consulted were primarily those involved in the development and implementation of the ocean physics parameterisations in that model. Over 35 experts were involved in the consultation process, which identified the uncertainty range for 16 different ocean parameters. A prioritisation of the different parameter perturbations was also established based on experience from prior sensitivity and tuning experiments. The complete results of this exercise are included in the appendix to aid future work using perturbing ocean parameters.

A relatively large amount of computer resources were allocated to create the experimental perturbed physics ensemble: a significant portion of the UK Met Office's access to the ECMWF machine [which was the 11th fastest supercomputer in the world at the time of allocation, (Top500.org 2004)]. These resources allowed for approximately 5,000 years of model integration with HadCM3. A trade-off was therefore required between ensemble size and spin-up time for each member. Collins et al. (2006) used flux-adjustments to partially reduce the spin-up time for their simulations with atmosphere perturbations. However, flux-adjustments are known to affect the simulation of the ocean state (Marotzke and Stone 1995) so they were not used in this initial study. Parameter perturbations can take thousands of years to fully affect the deep ocean (Stouffer and Manabe 2003); however having multiple spin-ups on these timescales would have severely limited the number of parameters perturbed. As a compromise, a spin-up period of 500 years for each perturbation was used, which is of the order of magnitude of many coupled model spin-ups (Randall et al. 2007). The deep ocean will still not have reached equilibrium after this spin-up time, yet it allowed a total of 7 experiments, rather the 3 permitted by a 1,000 year spin-up. Although a lack of equilibrium is far from desirable, it is not thought to impact the main results shown in this paper. Impacts of residual drift on precise details of the results cannot, however, be completely discounted.

The expert consultation found three parameters to be a high priority, so the ensemble consists of a maximum, minimum and an intermediate value for each of these parameters (Table 1). For two of the three parameters, the standard HadCM3 setting falls near the centre of the range, so is used as the intermediate value. This is not the case for the pair of mixed layer parameters, where the standard settings form the upper bound. Each ensemble member was initiated from the analysed temperature and salinity observations of Levitus and Boyer (1994), the sea ice observations of Rayner et al. (2003), a state of no motion and preindustrial levels of CO_2. After 500 years, they were deemed to have reached a quasi-stable state (this is true for the surface climate, but there is still some climate drift in the deep ocean, see Fig. 1 of C&07). An idealised climate change experiment was performed from this state, consisting of an 80-year simulation in which CO_2 levels increased by 1% per annum and a simultaneous 80-year control run with constant CO_2 levels.

While this study may be considered an initial sensitivity study to perturbed parameters in HadCM3, it would be detrimental to include members with too-unrealistic climates within the ensemble. As HadCM3 has been somewhat optimised during its development to provide, by some measures, the "best" simulation for the STD setup,

Table 1 Ocean model parameters used in the perturbed physics ensemble experiments and key quantities that determine the rate of global warming (adapted from Collins et al. 2007)

| | Isopycnal diffusivity ($m^2\ s^{-1}$) | Background vertical diffusivity profile ($\times 10^{-5}\ m^2\ s^{-1}$) | Mixed-layer parameters | | TCR $\sigma = 0.04$ (K) | λ $\sigma = 0.02$ ($Wm^2\ K^{-1}$) | κ $\sigma = 0.02$ ($Wm^2\ K^{-1}$) |
			Fraction	Depth (m)			
STD	1,000	1–15	0.7	100	2.07	1.17	0.63
LowISO	200	1–15	0.7	100	2.17	1.14	0.57
HighISO	2,000	1–15	0.7	100	2.07	1.19	0.61
LowLAM	1,000	1–15	0.3	100	2.16	1.16	0.57
MedLAM	1,000	1–15	0.5	50	2.11	1.14	0.69
LowVDIFF	1,000	0.5–4	0.7	100	2.28	1.07	0.55
HighVDIFF	1,000	2–50	0.7	100	1.82	1.31	0.74
Atmosphere physics (range)					1.56–2.61	0.85–1.75	0.57–0.76

The first column indicates the experiment name. The along-isopycnal diffusion coefficient takes a constant value everywhere in HadCM3 and is indicated in the second column. The background vertical diffusivity (third column) has a vertical profile with the first number in the column indicating the surface value and the second the value at the bottom of the ocean (see Table A of Gordon et al. 2000). The HadCM3 mixed-layer scheme is based on Kraus and Turner (1967). It has two interdependent parameters: a wind-mixing fraction (fourth column) and a decay depth (fifth column). The wind-mixing fraction scales the wind-mixing energy, which is calculated by the model at 10 m to give a surface value. The decay depth parameter determines the amount of wind-mixing energy that penetrates from the surface by controlling the rate of exponent decay. All these parameters are known to control processes responsible for vertical heat transport in ocean models. The sixth column gives the TCR, the 20-year averaged global mean temperature change at the time of CO_2 doubling in the 1% per year CO_2 increase experiment. The seventh column gives the effective atmospheric feedback parameter and the eighth column the ocean heat uptake parameter (see Collins et al. (2007) for information on how these are calculated). For the last three columns, the standard deviation in the calculation expected from natural variability (computed from all the control experiments) is shown. The values in some columns are shown to 2 decimal places to highlight small differences

Fig. 1 The average global mean depth profiles of the control simulations of the seven ensemble members. All of the profiles are presented as anomalies from the ensemble mean profile. The panels show the potential temperature, salinity and potential density from *left to right*
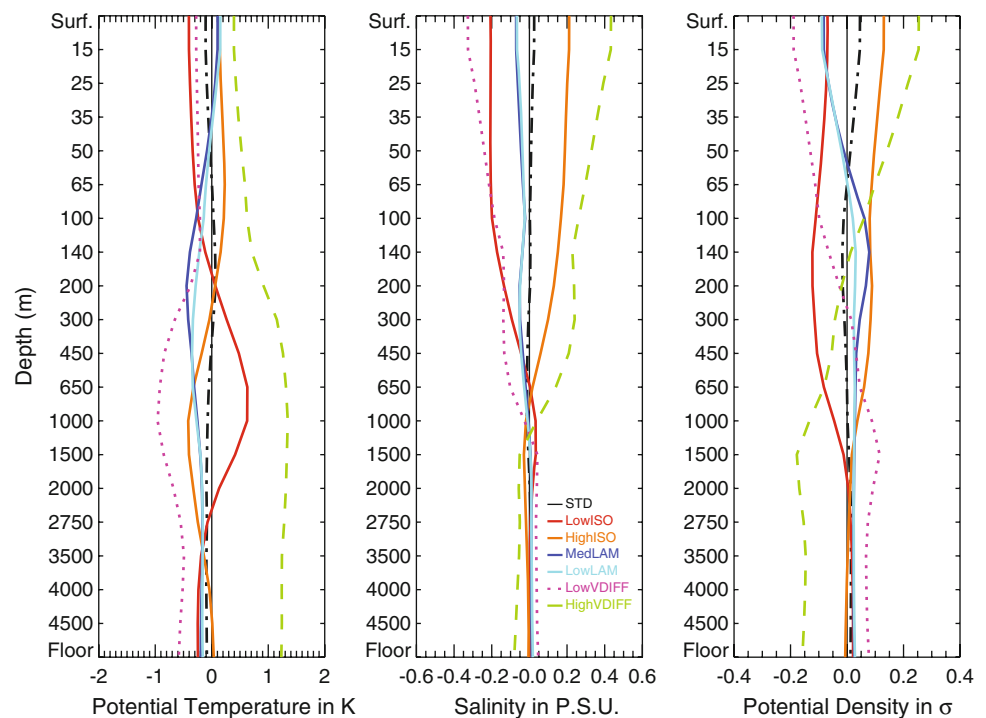
any parameter perturbation may be expected to degrade its climate simulation (although improvements in some fields are possible—see Table 2 later). It would be possible to combine multiple perturbations in an attempt to avoid degradation either using parameter estimation (Hargreaves et al. 2004) or knowledge from previous experiments (Webb et al. 2006). Unfortunately the validation of numerical models and their climate properties is a complicated task. There is no simple, objective way of determining the difference between a "good" model and a

"bad" model. Quantitative methods have been suggested (e.g. the climate prediction index of Murphy et al. 2004 or the Taylor-diagram of Taylor 2001 yet these still require expert judgement in setting the root-mean-squared-error thresholds, below which a model is acceptable.

The Intergovernmental Panel on Climate Change (IPCC) included projections from a variety of climate models in their fourth assessment report (AR4). Using a simple measure (the area-averaged root-mean-squared error of the modelled climate from observed datasets), the surface properties of each perturbed-physics ensemble member falls within the range from the climate models included in AR4 for at least one dataset (Table 2). The surface air temperature of High VDIFF is outside the AR4 range when comparing to the CRU $5° \times 5°$ dataset, but within the AR4 range when using the Legates and Willmott (1990) $0.5° \times 0.5°$ dataset. (Despite this, the High VDIFF ensemble member has an area-averaged root-mean-squared error in precipitation less than that of the standard model.) Based on this comparison, we choose to examine every ensemble member in the following analysis.

3 Previous findings

Quantifying the uncertainty in climate predictions has been an emergent field in the past decade. There have been a variety of approaches taken, which can be categorized by their different use of limited computing resources. Some authors have chosen to use simplified (and therefore computationally inexpensive) models to comprehensively investigate the uncertainty contained in parameters such as climate sensitivity (which are emergent properties of more complex models). For example, both Wigley and Raper (2001) and Forest et al. (2002) show that uncertainties in the rate of ocean heat uptake have less impact on the predicted global mean temperature than climate sensitivity and forcing uncertainties.

By using more sophisticated sampling methods, the computational expense of comprehensively sampling parameter space can be reduced. Hargreaves et al. (2004) sample with an ensemble Kalman filter, which allows them to incorporate a 3D ocean model into their study. They predict a transient climate response (TCR, defined

Table 2 A comparison of the preindustrial climates to observations for a variety of variables

Variable	Obs.	STD	Low ISO	High ISO	Med LAM	Low LAM	Low VDIFF	High VDIFF	AR4 Range
1.5 m temp. (°C)	CRU	2.55	2.32	2.78	2.72	2.77	2.46	**3.03**	1.61–2.82
1.5 m temp. (°C)	Legates/Willmot	3.71	3.53	3.85	3.78	3.80	3.61	4.03	3.07–4.45
Precip. (mm/day)	CMAP	1.60	1.62	1.60	1.49	1.50	1.68	1.50	1.10–1.86
Precip. (mm/day)	Legates/Willmot	1.76	1.79	1.75	1.69	1.69	1.84	1.66	1.41–2.04
Surf. Press. (Pa)	HadSLP2	435	436	436	437	435	440	430	
OLR (Wm^{-2})	ERBE	13.4	13.1	13.7	13.6	13.6	13.4	13.7	
TOA Flux (Wm^{-2})	ERBE	12.4	12.5	12.4	12.1	12.1	13.0	11.4	
SST (°C)	Levitus	2.03	1.86	2.20	2.16	2.19	1.94	**2.41**	
SST (°C)	HadISST	3.05	2.93	3.18	3.15	3.17	3.00	2.34	
SSS (psu)	Levitus	2.21	2.33	2.13	2.27	2.27	2.44	2.07	
Ocean θ (°C)	Levitus	1.22	**1.37**	1.18	1.17	1.18	1.19	**2.05**	
Ocean Sal. (psu)	Levitus	0.47	0.49	0.45	0.49	0.49	0.51	0.43	
ACC (Sv)	*123–135*	218	235	208	228	227	220	218	*34–336*
MOC (Sv)	*15–20*	19	18	18	18	19	17	25	*5–36*
10 year Var. of MOC (Sv)		0.8	0.5	0.5	0.5	0.4	0.5	0.7	
Interannual var. of GM SAT (°C)	*0.12*	0.14	0.14	0.13	0.17	0.15	0.14	0.12	

The values shown are the global root-mean-squared error of the 80-year mean of the control simulation compared to an observed data source. The AR4 range for the Antarctic circumpolar current (*ACC*) and the meridional overturning circulation (*MOC*) are taken from Russell et al. (2006). The CRU dataset is documented by Jones et al. (1999); the Legates/Willmot dataset by Legates and Willmott (1990); CMAP by Xie and Arkin (1996); HadSLP2 by Allan and Ansell (2006); ERBE by Barkstrom (1984); Levitus by Levitus and Boyer (1994); HadISST by Rayner et al. (2003). The ACC observations were made by Whitworth and Petersen (1985) and Cunningham et al. (2003). The MOC observations are presented in Schmitz (1996) and Bryden et al. (2005). The interannual variability of the global mean surface temperature is computed from the GISST dataset of Hansen et al. (1999)

If a value is shown in *italics*, it is the average value of the variable in the control simulation (in these cases observed values are shown rather than a data source)

Bold font means that the difference between the ensemble member's root-mean-squared error and STD's is greater than 10% of STD's root-mean-squared error. All the root-mean-squared errors are area or volume averaged as appropriate

as the global mean temperature at the time of CO_2 doubling in a 1% per annum increasing CO_2 scenario by Cubasch et al. 2001) of $1.6 \pm 0.04°C$. This spread in TCR is markedly lower than suggested by the spread of models included the IPCC reports, however they produce a large spread in Atlantic meridional overturning circulation (Hargreaves et al. 2004). Inclusion of a more complex atmosphere model is expected to dramatically enhance the spread of their prediction, as the results from Wigley and Raper (2001), Forest et al. (2002) and C&07 indicate.

A complex 3D atmosphere model can be used, but a much less exhaustive sampling of parameter space must be used to compensate for the additional computational expense of running the model (e.g. Murphy et al. 2004, Stainforth et al. 2005). Subsequent studies have used a sub-sample of these results and incorporated a complex ocean model as a step towards creating transient regional predictions (Collins et al. 2006 and Harris et al. 2006).

C&07 described global mean results from the seven-member perturbed ocean parameter ensemble described in the previous section. Table 1 shows the TCR, climate sensitivity (λ) and ocean heat uptake efficiency (κ) presented in C&07 for each ensemble member. Table 1 also shows the results for a perturbed atmosphere parameter ensemble (Collins et al. 2006). It can be seen that impact of ocean perturbations on the climate sensitivity is less than the impact of the atmosphere perturbations, which is to be expected as the climate sensitivity is dominated by atmospheric and surface processes. However, the atmosphere perturbations cause a similar range in ocean heat uptake efficiency (defined by Gregory and Mitchell (1997) to have equivalent units as the climate sensitivity) as the ocean perturbations: implying that the ocean perturbations have only a limited impact on the ocean heat uptake.

C&07 make no attempt to explain, in detail, the limited impact of ocean parameter perturbations, instead they just speculate on possible causes. Previous sensitivity studies for the individual parameters have shown some significant impacts on climate change in other models (e.g. Dalan et al. 2005a and Gnanadesikan et al. 2005). However, few sensitivity studies which aim to stay within the realistic bounds of the parameter have been performed, and none of those use HadCM3. HadCM3 consists of a $2.5° \times 3.75°$, 19 sigma level atmosphere model, a sophisticated land-surface scheme, a zero-layer sea ice model as well as the ocean model (Gordon et al. 2000). The ocean component is a $1.25° \times 1.25°$ gridpoint model with 20 fixed depth levels and a rigid lid. This model has previously been used interpret observed ocean heat uptake (Gregory et al. 2006 and Barnett et al. 2005).

4 Why is the ocean heat uptake relatively insensitive to ocean parameter perturbations?

The surprising result of C&07 was that variations in the rate of ocean heat uptake in the perturbed ocean parameter ensemble (as measured by the ocean heat uptake efficiency) cause similar spread in TCR as variations in the climate sensitivity. In fact, an ensemble sampling purely atmosphere parameter uncertainty produces a similar range of variations in ocean heat uptake efficiency. This section aims to understand and explain the lack of influence of ocean parameter perturbations on the global mean ocean heat uptake found by C&07 in the HadCM3 ensemble. The global mean temperature, salinity and potential density profiles will be presented, but the majority of the analysis will focus on the heat transfer diagnosed from different physical processes.

The rate of potential temperature change from each parameterisation at each grid point in the ocean can be stored during a HadCM3 integration. These heating rates can be used to calculate a global mean vertical heat flux between model levels,

$$F(Z) = \rho c_p \left\langle \int_{-H}^{Z} \frac{d\theta}{dt} dz \right\rangle_{\text{Globe}} \quad (1)$$

where ρ is the average density of sea water (taken to be 1,026 kgm^{-3}), c_p is the specific heat capacity of water at a constant pressure (3,988 $Jkg^{-1}°C^{-1}$), $d\theta/dt$ is the diagnosed heating rate (computed at each time and subsequently averaged), $\int_{-H}^{Z} dz$ is the vertical integral from the bottom of the ocean up to level z and $\langle\rangle_{\text{Globe}}$ is the horizontal average over the whole globe. These diagnostics were introduced by Gregory (2000) and used to investigate the heat budget of HadCM2; the previous generation of the model.

4.1 Global mean vertical heat budgets in the baseline control climates

The ocean parameter perturbations alter the simulation of the climate state throughout the depth of the ocean. This can be seen in Fig. 1, which shows changes in global mean ocean profiles. Each ensemble member's potential temperature, salinity and potential density are expressed as anomalies from the ensemble mean profiles. The vertical coordinate is linear in model level, rather than depth, to emphasise the upper ocean changes. The STD model version happens to be very similar to the ensemble mean, so the differences shown can also be considered as the impact of each parameter change.

All of the parameter perturbations change the surface density. A perturbed diffusivity (either isopycnal or background vertical) causes competing changes in salinity and

temperature, yet the change in salinity always dominates the change in surface density. The reduction in surface density with the mixed-layer perturbations derives from both cooling and salinification of the surface, rather than opposing changes. This was to be expected as the mixed-layer scheme (Kraus and Turner 1967) acts only on potential density of the water column, rather than potential temperature and salinity separately. Both the mixed-layer perturbations appear to reduce the global efficiency of surface mixing, as the surface lightens whilst the density below 100 m increases (at the base of the mixed layer). This represents a steepening in the global mean pycnocline consistent with a shallower mixed layer.

The total salt content of the ocean is approximately constant. Therefore, if a parameter perturbation causes an increase in salinity at one location, then there must be a compensating reduction elsewhere. The impact on temperature need not be compensatory as heat can be supplied or removed at the surface. Vertical diffusivity strongly influences the ocean temperature below 300 m. The temperature effect of the vertical diffusion perturbations reduces above this level, because the vertical diffusion plays a relatively minor role in the heat budget near the surface. Low VDIFF shows smaller changes in the deep ocean than High VDIFF, because the STD setting of vertical diffusivity means that there is already little influence of vertical diffusion at these depths. These impacts are consistent with results of Dalan et al. (2005b), who perturbed the vertical diffusivity in an earth system model of intermediate complexity (EMIC).

Perturbations to the isopycnal diffusivity bring about persistent change in the potential density down to 1,500 m (after which they are much smaller). Superficially this is surprising, as isopycnal diffusion only occurs along lines of constant density by definition. However, separate diffusion of salt and temperature along isopycnals can lead to resultant water masses with different densities. Near the surface these density changes are dominated by salinity, but temperature anomalies play a greater role at depth. Increased isopycnal diffusion leads to a warmer surface, at the expense of the ocean interior, implying that the net impact of isopycnal diffusivity is a cooling of the interior of the ocean (as found by Gregory 2000 and Huang et al. 2003b). This can be investigated more exactly by using the diagnostics defined in Eq. 1, which are shown in Fig. 2.

In the ensemble mean (Fig. 2, top left panel) both vertical diffusion and advection cause a downward heat flux at all depths. The concept of a global mean advective heat flux is discussed in more detail in Gregory (2000), but can be thought of as the effect of water being advected downwards being warmer than water in the return flow. In equilibrium, this downward heat flux must be balanced by an upward heat flux from other processes; namely isopycnal diffusion, convection, mixed layer physics and the thickness diffusion of Gent and McWilliams (1990), henceforth termed the GM flux. These six processes combine to characterise the heat budget below the surface layer. Other processes such as the penetration of solar radiation and the surface heat fluxes will affect the surface layers and they are included as "Other" in Fig. 2. Their impact below 50 m is negligible in comparison with the other vertical heat fluxes.

A very similar heat balance also exists in the STD model's baseline climate, as the anomalies between it and the ensemble mean (shown in the top right) are much less than the other ensemble members. This general heat balance is similar to that seen by Gregory (2000) in the previous generation of the Hadley Centre model (HadCM2), but with some variation in the specific depths at which processes dominate. This heat balance is also consistent with the results of Dalan et al. (2005b), whose intermediate-complexity model does not have an equivalent mixed layer.

Isopycnal diffusion causes an upward flux of heat (against the global mean vertical temperature gradient) because of sloping isopycnals in high latitudes, where the salinity dominates the density calculation. The GM flux is the largest upward vertical heat flux below 100 m in the ensemble global mean and is also caused by the sloping isopycnals in high latitudes. The convective parameterisation operates infrequently and at limited locations, so has a small effect on the global-mean heat balance, although it causes large heat transfers locally. The mixed layer parameterisation acts to bring heat up to the surface in the global mean. At times when the sea surface is warmer than the air above (e.g. winter, night), the ocean will lose heat from the sea surface to the atmosphere. This surface heat loss causes the surface water to become denser and sink, to be replaced by warmer water from deeper within the mixed layer. None of the ensemble members have reached a complete equilibrium throughout the ocean, as can be seen by the existence of a "total imbalance" in each member. The imbalance is most notable in the vertical diffusivity perturbations and would lead to an enhancement of the temperature anomalies shown at depth in Fig. 1.

The six lower panels in Fig. 2 show each ensemble member's heat balance. It can be clearly seen that the perturbations to each parameter change the vertical heat flux from that parameterisation. As would be expected near equilibrium, the heat flux change from the perturbed process is balanced by changes from other processes. Most of these compensation mechanisms can be explained using simple oceanographic models. For example, the shallower mixed layer indicated in Fig. 1 means that there is less upward heat flux in the region of its original base, and more at its new base. A shallower mixed layer would also mean a sharper thermocline, and so there would be a higher

Fig. 2 The global mean profile of the vertical heat flux from different ocean physical processes. The *top right panel* shows the ensemble mean profile, *top right* shows the difference between the STD and ensemble mean, whilst the other panels show the deviations of single ensemble members from the ensemble-mean profile. The *grey line* indicates the transition between the seasonally-affected surface waters and the ocean interior (as determined by Gregory 2000)
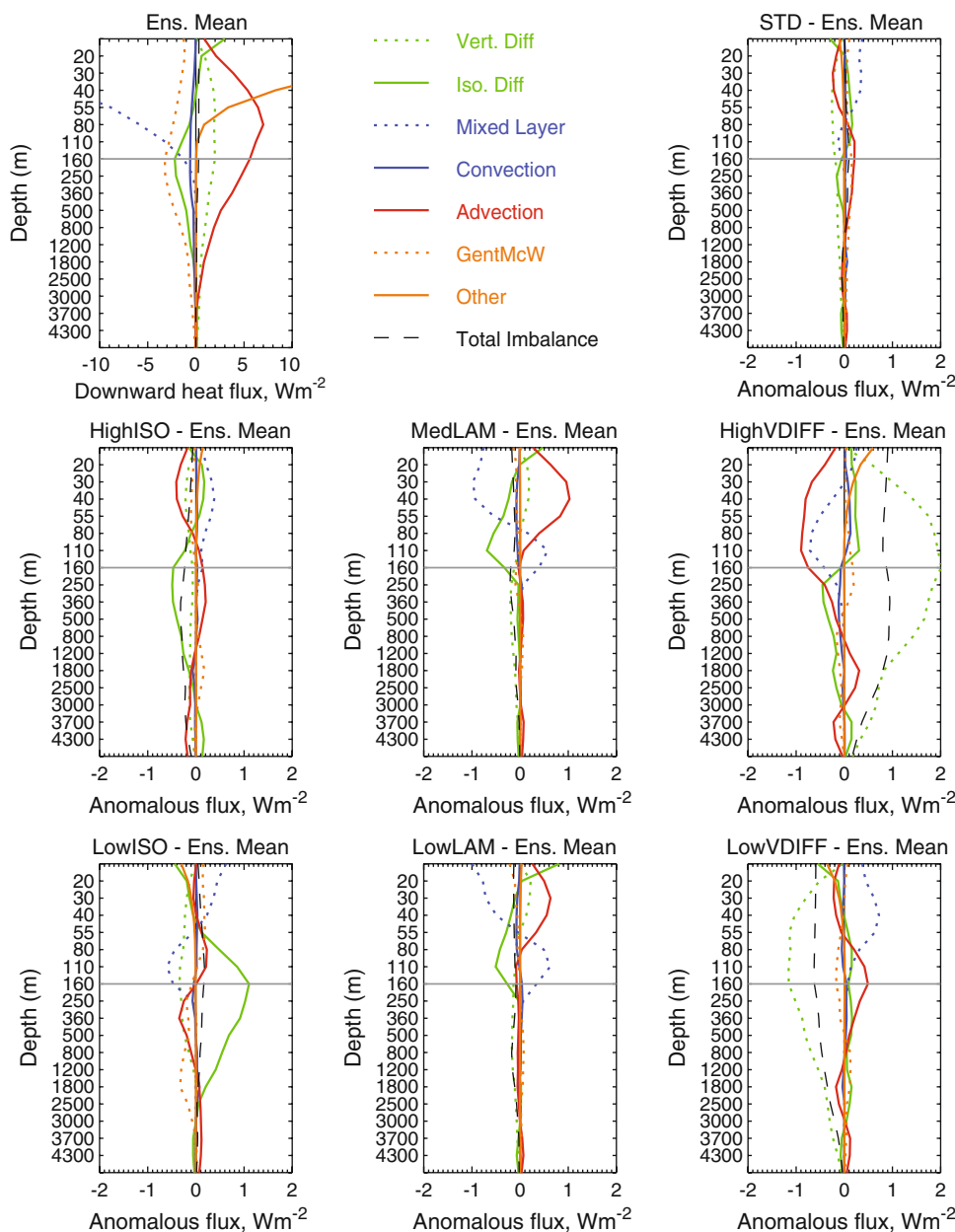
advective heat flux generated by moving the same amount of water across this stronger gradient. The shoaling of the mixed layer also leads to cooler water at its old base (Fig. 1), which creates greater vertical gradients along the isopycnals, and thus an increase in the upwards isopycnal heat flux. The vertical diffusivity perturbations cannot be explained simply with a global mean analysis, partly because compensating processes change depth and magnitude between the HighVDIFF and LowVDIFF runs.

4.2 Ocean heat uptake under increasing CO_2

The primary role of the ocean in transient climate change is its large potential for heat uptake. It was shown by C&07

that the ocean heat uptake efficiency (a global mean diagnostic devised by Gregory and Mitchell 1997) varies across the perturbed ocean parameter ensemble, but that these changes are similar in magnitude to an ensemble without ocean parameter perturbations. C&07 also noted that the variations in ocean heat uptake efficiency account for only half of the variation in transient climate response seen in the ensemble. Evidence was presented above which shows the parameter perturbations alter the baseline vertical energy budget of the ocean. Therefore, one could expect the parameter perturbations to alter the ocean heat uptake under climate change, yet C&07 show the variations are relatively unimportant. In this section, we compare two possible explanations for C&07's result; firstly that

parameter perturbations may only weakly influence the ocean heat uptake of a parameterisation scheme, and secondly that there may be compensatory changes that reduce the direct impact of a parameter perturbation.

Figure 3 shows the global mean depth profiles of anomalies in the climate change signal in potential temperature (left), salinity (middle) and potential density (right): the deviation of each member from the ensemble mean climate change signal is plotted. Where there are positive deviations at one depth and negative deviations at another depth, we may say that there is some compensation of changes with depth. Examples of such depth compensation should occur in the salinity profile, because the total salt content of the ocean remains approximately constant on centennial time scales. However, there is also depth compensation in the potential temperature profiles. This is most obvious in the case of the HighVDIFF perturbation, but all ensemble members show some kind of depth compensation with either positive anomalies overlying negative anomalies, or vice-versa. Depth compensation reduces the variations in total ocean heat uptake seen in the ensemble. (In the extreme case of exact compensation, the total ocean heat uptake would be constant, but this does not occur here, as shown by C&07.)

The change in global mean downward heat fluxes for the different perturbations from the different physical processes is presented in Fig. 4 (calculated using Eq. 1). The top left hand panel of Fig. 4 show the STD model's climate change signal in these fluxes. The symbols indicate an anomaly that is statistically distinguishable from internal

variability, as determined from 20 year segments of the combined ensemble control runs (significance testing was not possible in Fig. 2 as the required diagnostics from the millennia-long HadCM3 control are not available).

During transient climate change, the mixed layer scheme is responsible for most of the additional downwards heat transfer in the top 160 m of the ocean. Advection then dominates until 350 m. The isopycnal diffusion dominates the vertical heat transfer below 350 m until 1,500 m. The additional heat content from an increase in CO_2 is minimal below this depth. This is a similar order of dominance as found by Gregory (2000) in the previous, lower-resolution version of the model, however the transitions occur at different heights. The EMIC used by Huang et al. (2003a, b) and Dalan et al. (2005a, b) has much less resolution near the surface and no mixed-layer scheme. Therefore, the partitioning seen in their studies differs from that shown here.

One possible explanation for the small range of ocean heat uptake in C&07 is that the ocean model is insensitive to the parameter perturbations that were applied. This appears not to be the case, as even the weakest perturbation causes a maximum change of that parameterisation's flux (shown in Fig. 2) that is at least one-third of STD's climate change signal at that depth.

The climate change signal in global mean downward heat fluxes for each individual ensemble member are shown as the other panels in Fig. 4. They are shown as anomalies from the STD-member climate change signal. (In this case there are some significant differences between

Fig. 3 The global mean depth profiles of the climate change signal. They are shown as deviations from the ensemble mean change. The *panels* show the potential temperature, salinity and potential density from *left to right*
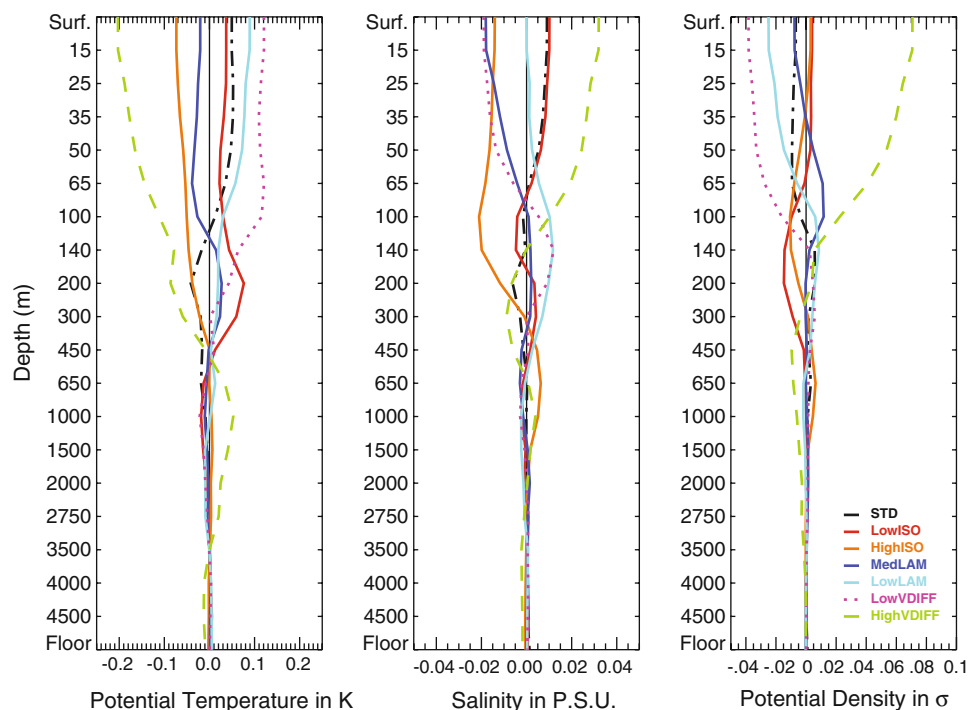
Fig. 4 The variations in the changes of the global mean vertical heat transfers at the time of CO_2 doubling. The STD member signal is shown in the *top left panel*; *top-right* shows the difference between the ensemble mean and the STD. The ensemble members are shown as deviations from the STD. A *symbol* indicates that the deviation is significantly different from that expected by natural variability at the 5% level
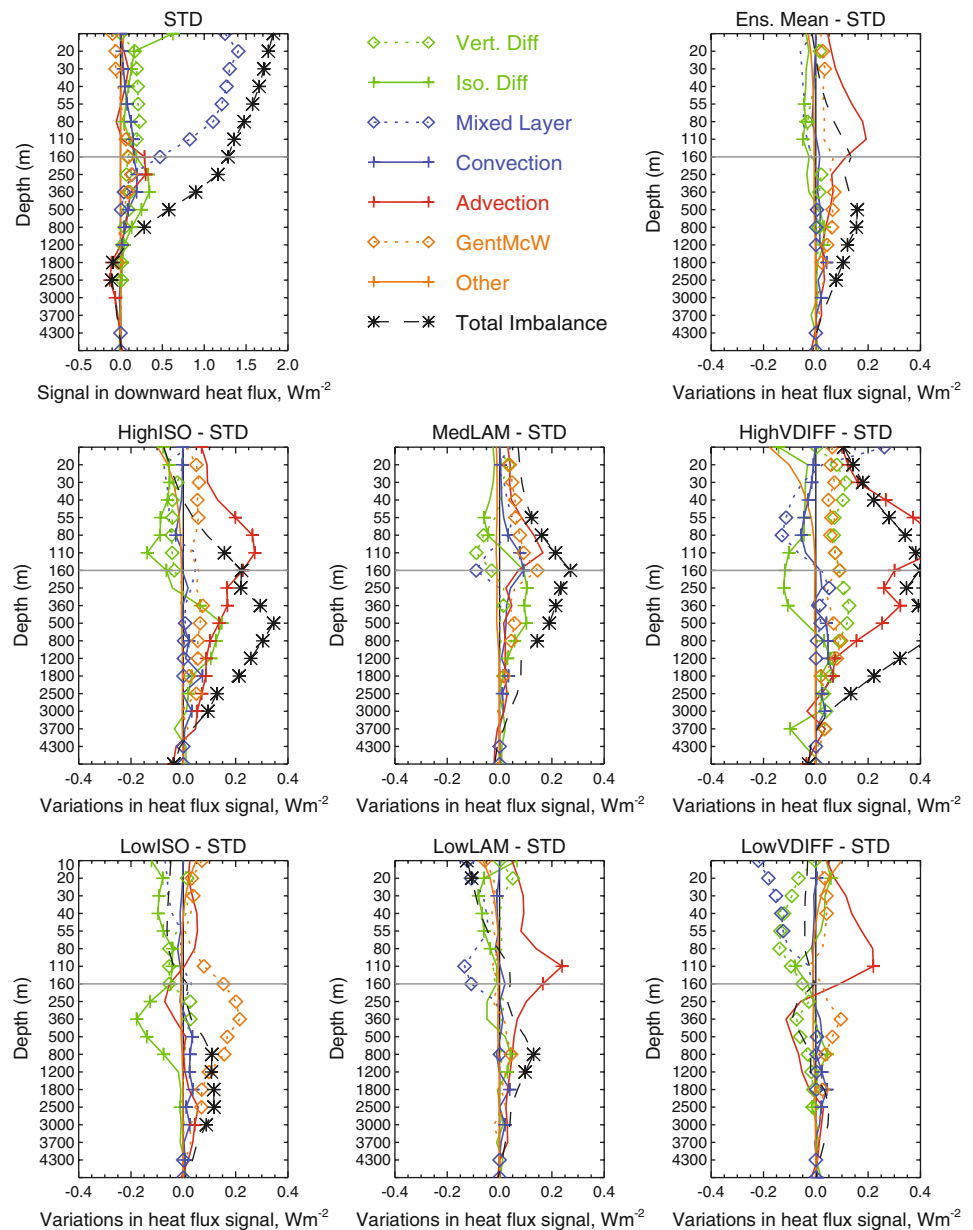
the behaviour of the STD model and the ensemble mean.) We discuss the changes in the individual members with respect to the STD to emphasise the exact role of the parameter perturbations.

It is worth noting here that, in contrast to the case of the quasi-equilibrium control experiments, the vertical heat transports have not equilibrated and the ocean would continue to warm if the CO_2 forcing were to be held fixed from this point in the experiments. Hence we would not, a priori, expect the kind of compensation of heat transports that is evident in Fig. 2 where the experiments are approaching a quasi-equilibrium state. It would be quite possible to see changes in a single heat transport process which, when others remain unperturbed, would result in a

different rate of total heat uptake and transient climate change.

Figure 4 shows that there are significant compensating changes in the vertical heat fluxes, despite the above reasoning. It can be seen that the perturbed process is never affected by the parameter perturbation in isolation: there are always significant changes from unperturbed processes. Our findings show a degree of similarity to the results of previous studies, although they are somewhat difficult to interpret. Huang et al. (2003a) found that the ocean heat uptake is insensitive to perturbations in the isopycnal diffusivity, because of compensation from other oceanic processes. These results support that conclusion. Dalan et al. (2005a) found that perturbations to the vertical

diffusivity cause significant variations in the ocean heat uptake. LowVDIFF is the only member of this ensemble that shows no significant changes in the total vertical heat flux (no black crosses, just a black line in Fig. 4). Yet the increased vertical diffusivity (HighVDIFF) shows the largest changes of any ensemble member.

The mixed layer perturbations both show only small changes in the mixed layer heat flux, but variations in other processes create significant changes in the total vertical heat flux. These variations probably arise from the impact of the parameter perturbation on the baseline state, rather than any transient processes. The isopycnal perturbations are noteworthy in that both HighISO and LowISO have significantly higher total vertical heat flux below 800 m. Whilst this is dominated by an increase in isopycnal diffusion in HighISO, in LowISO the higher flux is created by corresponding changes in the GM flux (which was perturbed as well as the diapycnal diffusivity in Dalan et al. 2005a, b).

The impacts of the vertical diffusivity perturbations exemplify the complex interconnections between processes in the ocean model. LowVDIFF shows a significant reduction in the vertical heat flux from vertical diffusion, which is compensated for by advection and GM flux at different levels. However, HighVDIFF has an increase in heat flux from vertical diffusion that is reinforced and amplified by those two same processes. These two ensemble members determine the range of ocean heat uptake efficiency (κ, Gregory and Mitchell 1997) seen by C&07 and presented in Table 1, yet the total rate of heat flux in LowVDIFF is not statistically distinguishable from the STD member. This is possible as the ocean heat uptake efficiency is defined as the change in heat flux divided by the TCR, and there are significant differences between the TCR of LowVDIFF and STD.

4.3 Summary of global mean heat uptake findings

This section set out to explain the relative insensitivity of the ocean heat uptake efficiency to ocean parameter perturbations. There is no single overarching explanation identified by the analysis presented above. It is clear that the parameter perturbations definitely have the expected direct impacts on the climate-change-induced vertical heat fluxes calculated by the parameterisations. However, these direct impacts are relatively small on the global scale (for example the mixed layer perturbations change the mixed layer heat flux by only 10% of the total rate of heat uptake at the depth of their greatest impact). More interestingly though the direct impacts are also modified by ocean interactions that cause changes in vertical heat fluxes from unperturbed processes. There appears to always be some compensation between the processes leading to a reduction

of the changes in heat flux, and hence ocean heat uptake. It is likely that the majority of the changes in the ocean heat uptake occur from changes in the baseline climates caused by the parameter perturbations (agreeing with the finding of Dalan et al. 2005a). We have presented a global mean analysis, but as no single explanation arises, a regional analysis for each ensemble member would need to be undertaken to determine the exact mechanism for the insensitivity to that parameter perturbation.

It is clear from Fig. 2 that the deep ocean is not fully equilibrated by the beginning of the increasing CO_2 experiment in the experiments with vertical diffusivity perturbations. The impact of the residual climate drift in these simulations is hard to estimate quantitatively. The definition of the climate change signal as the contemporaneous difference between the two model runs acts to remove some of the impact of climate drift. The method assumes that the residual climate drift and the climate change signal are completely independent. The only possible method to truly remove any effects of climate drift from the simulation would be to integrate the baseline simulations longer, which unfortunately was not feasible. HighVDIFF has both a largest anomalous signal and largest drift. The member with the next largest drift, LowVDIFF actually has no significant anomalies in its climate signal, rather than amplified anomalies. One could take this as evidence that the amount of residual climate drift does not impact the perturbed response to the imposed forcing.

5 Does ocean parameter uncertainty impact regional climate change predictions?

The main purpose for creating the perturbed ocean parameter ensemble analysed here was to begin investigating the importance of ocean parameter uncertainty in probabilistic predictions of climate change. C&07, and the analysis presented above, show that ocean parameter uncertainty is not as important as atmosphere parameter uncertainty in determining global mean properties. However, many locations will not experience global-mean climate change. This latter half of the paper investigates the extent to which a probabilistic regional climate forecasting system needs to incorporate ocean parameter uncertainty to correctly sample uncertainties in regional climate changes.

In addition, we also examine the Atlantic meridional overturning circulation; a feature of the climate system that has received much attention recently with both observations and modelling studies (e.g. Bryden et al. 2005, Gregory et al. 2005). It is expected to be especially responsive to ocean parameter perturbations (Hargreaves et al. 2004), so is investigated in Sect. 5.4.

5.1 Regional structure in the baseline surface simulation

The spatial patterns of baseline, pre-industrial climates will be discussed before looking at the spread in the climate change signals. The reasons for this are twofold; firstly a portion of variations in the climate change signal will be a consequence of these changes and secondly it should be easier to explain variations in the steady-state changes than the transient behaviour. Figure 5 compares the spatial patterns of the time-average surface air temperature (SAT, calculated at a height of 1.5 m) in the baseline climate across the ensemble. The top left panel shows the ensemble mean pattern and the other panels show the deviation from the mean pattern for each member. The deviations are only shown if they are significantly different from modelled internal variability at the 5% level when compared to a multi-millennia control simulation of HadCM3 (henceforth, these deviations will be termed "detectable").

Fig. 5 The average surface air temperature in the control simulations. The *top left panel* shows the ensemble mean pattern, whilst the other panels show the deviations from that pattern (where the differences are detectable from internal variability at the 5% level). On these deviation panels, *green* indicates a detectable change that has a magnitude of less than 0.25°C. The global mean temperature is shown in parentheses next to name of the ensemble member
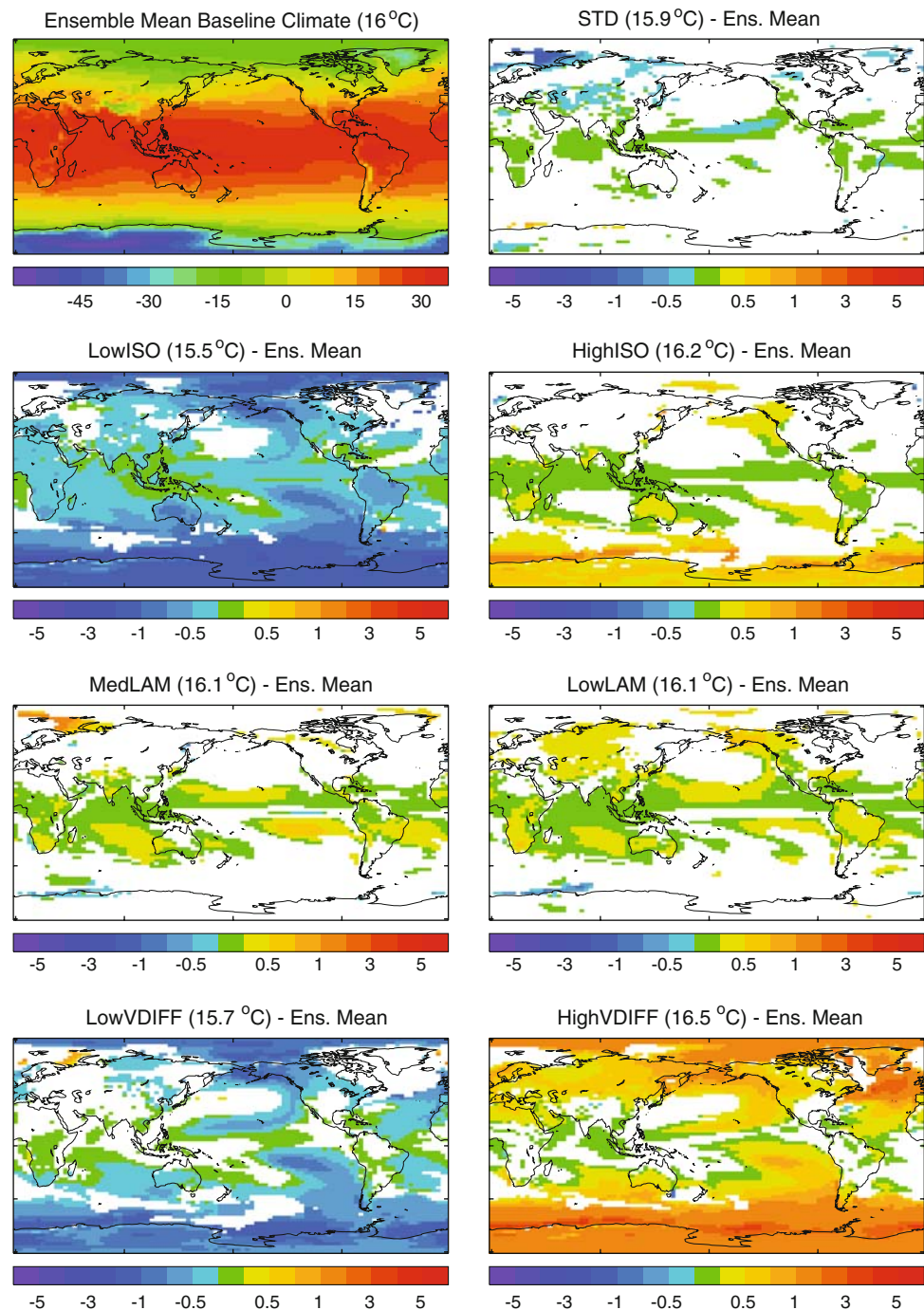
The STD simulation is very similar to the ensemble mean, with few significant SAT differences greater than 0.5°C. This partially reflects the experimental design which, in the case of perturbations to the isopycnal diffusion and vertical diffusivity, places the STD model near the centre of the distribution of parameters. It means that it is appropriate to consider variations in the perturbed members from the ensemble mean to also be representative of variations about the STD version of the model. The biases in modelled climate for the STD model are described in Gordon et al. (2000) and a comparison of each ensemble member to observations is shown in Table 2.

Each parameter perturbation causes detectable variations in the SAT climatology. These variations are not confined to the ocean, but also occur over the land for every parameter. As seen with the vertical profiles presented earlier, the two pairs of diffusivity perturbations cause the largest climate impacts. The surface patterns for these two pairs of parameters are approximately anti-symmetric (spatial correlations of −0.81 for the isopycnal diffusivity pair and −0.85 for the vertical diffusivity pair). All four diffusivity perturbations appear to have their maximum impacts in the high latitudes and in the gyre flow on the Eastern side of the basin.

The imposed perturbations to the mixed layer parameters were not symmetric about the STD model as the two parameters perturbed have interacting and compensating effects. Detectable SAT differences from the ensemble mean/STD are evident in the tropical and subtropical regions and, in the case of LowLAM, extending to the mid-latitudes in some regions.

Figure 6 shows the ensemble range in the equilibrium baseline climate state for four surface variables. The ensemble range is chosen as a suitable measure of ensemble spread as the ensemble extends to the extreme value of the uncertainty range in each parameter, rather than sampling systematically within the uncertainty range (c.f. Murphy et al. 2004 and Webb et al. 2006). This will only give us information about the extent of uncertainty arising from these ocean model parameters, instead of a (prior) distribution which, in this case, would not be possible anyway because of the small ensemble size. This work is only an initial exploration to gauge the importance of such ocean model parameter uncertainty, so determining a maximum bound is sufficient for our purposes.

The ensemble spread in the SAT (Fig. 6a) is largest in high latitudes. The majority of the Southern, North Atlantic and Arctic oceans have a spread of greater than 2°C (demarked by the black contour), approaching 5°C in places. There are also distinctive "tongues" in the equatorward sections of the subtropical gyres, which have a spread of greater than 1°C. These tongues are possibly caused by advection of anomalies sourced in high latitudes by the gyre, causing spread in the local temperature. The sea surface temperature pattern (Fig. 6c) echoes the surface air temperature pattern, but without the large spread in the Arctic and surrounding the coast of Antarctica, because ice cover provides a cap on the sea surface.

There is less detectable spread in precipitation (Fig. 6b). The largest spread occurs on the equatorward edge of the tongues of surface temperature spread. These tongues occur between areas with very low precipitation and the

Fig. 6 The ensemble range in the average of the control simulation for a selection of variables. The panels are only shaded when the ensemble variance is significantly greater than the natural variance at the 5% confidence level
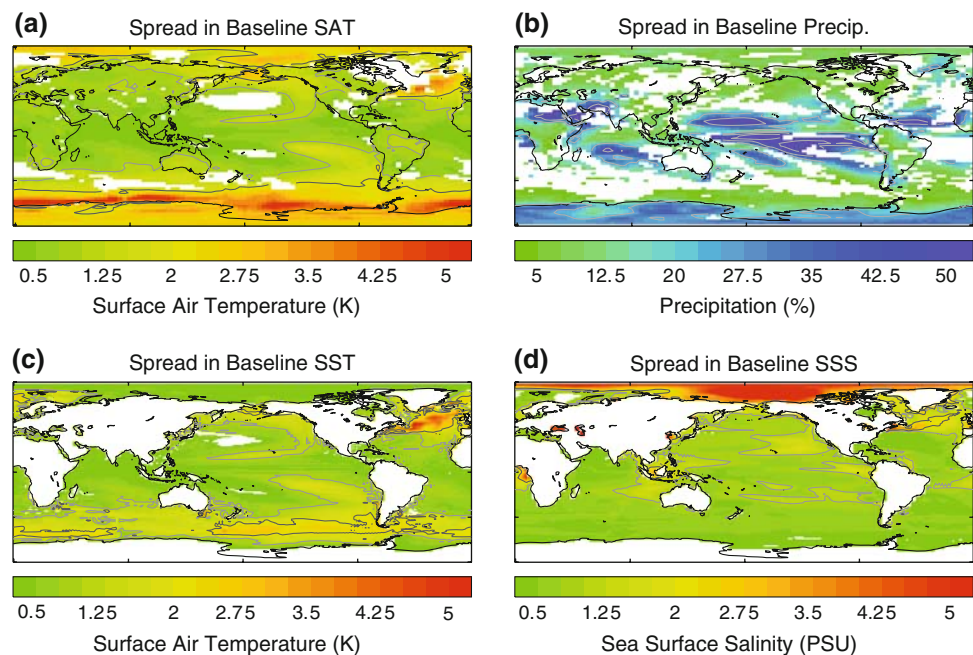
inter-tropical convergence zone (ITCZ) in the ensemble mean, so steep meridional precipitation gradient occurs in this region. Slight variations in the location and expanse of the ITCZ are consistent with the variations in the underlying SSTs.

The largest spread in sea-surface salinity (SSS, Fig. 6d) occurs in the Arctic Ocean, and is associated with spread in the sea ice volume (not shown, but also indicated by the large ensemble spread in surface air temperature in the region). The ensemble spread in SSS in the Southern Ocean is some of the smallest despite some spread in the sea ice. This discrepancy occurs as an increase in sea ice in the Southern Ocean leads primarily to an increase in sea ice area, whilst the area of the Arctic is constrained by the topography. Therefore the increase in sea ice in the Arctic results in an increase in ice depth and more concentrated local sea ice processes, such as brine rejection. There is also SSS spread in the regions of tropical convection (e.g. the maritime continent) related to the ensemble spread in precipitation, which although small as a percentage is large in absolute terms.

5.2 The spatial pattern of climate change signal

The ensemble mean climate change signal in surface air temperature, precipitation, sea surface temperature and sea surface salinity is shown in Fig. 7. We define the climate change signal for each ensemble member by taking the contemporaneous difference between the final 20 years of the 1% per annum simulation and the control simulation.

This time period is centred on the time of doubled CO_2 as in the definition of the transient climate response (e.g. Meehl et al. 2007, C&07). The ensemble mean surface temperature change is similar to that seen in other coupled models (e.g. Meehl et al. 2007) with polar amplification, an increased warming over the continents and warming minima over the Southern Ocean and in the North Atlantic. The climate change signal in precipitation is consistent with an enhanced hydrological cycle and is again similar to that shown in e.g. Meehl et al. (2007).

Figure 8 shows the surface air temperature climate change signal as anomalies from the ensemble mean pattern (shown in the top left panel). As with the baseline climate, differences between the ensemble mean surface air temperature climate change signal and STD are few, reflecting the experimental design of perturbing about the standard model setup. The impacts of isopycnal diffusion perturbations are only barely detectable. The LowLAM experiment causes significant differences over equatorial land regions, which are likely related to temperature variations over tropical oceans that have not passed the strict significance test. The vertical diffusivity perturbations cause widespread significant impacts and dominate the ensemble spread in the climate change signal.

5.3 Spread in the regional climate change signal

The ensemble spread in regional climate change signal is shown in Fig. 9. There is detectable regional ensemble spread covering the majority of the globe. The SAT spread

Fig. 7 The ensemble mean climate change signal in a selection of variables
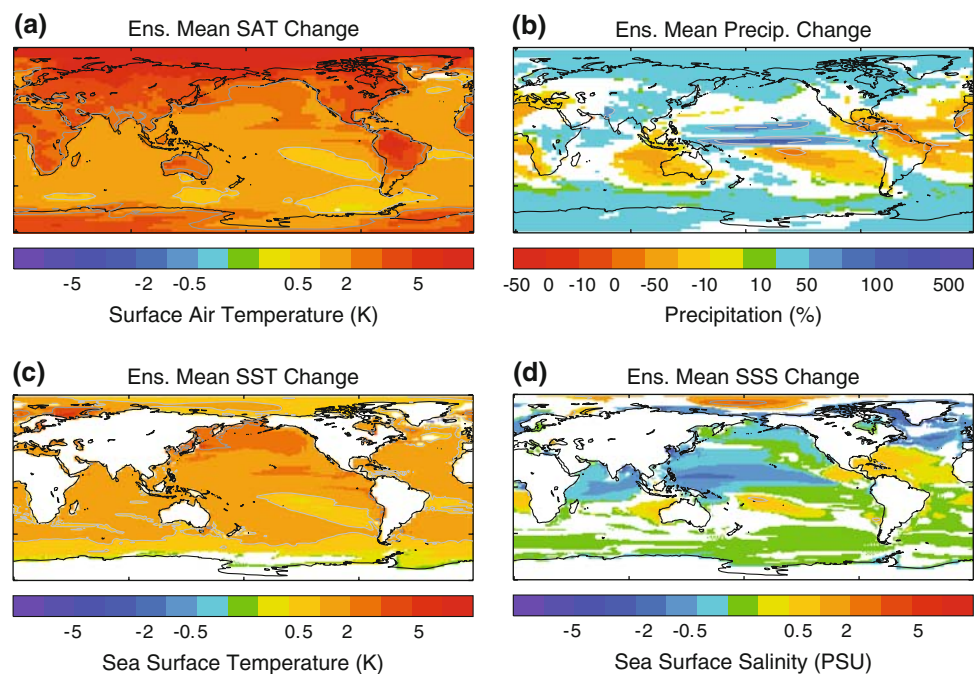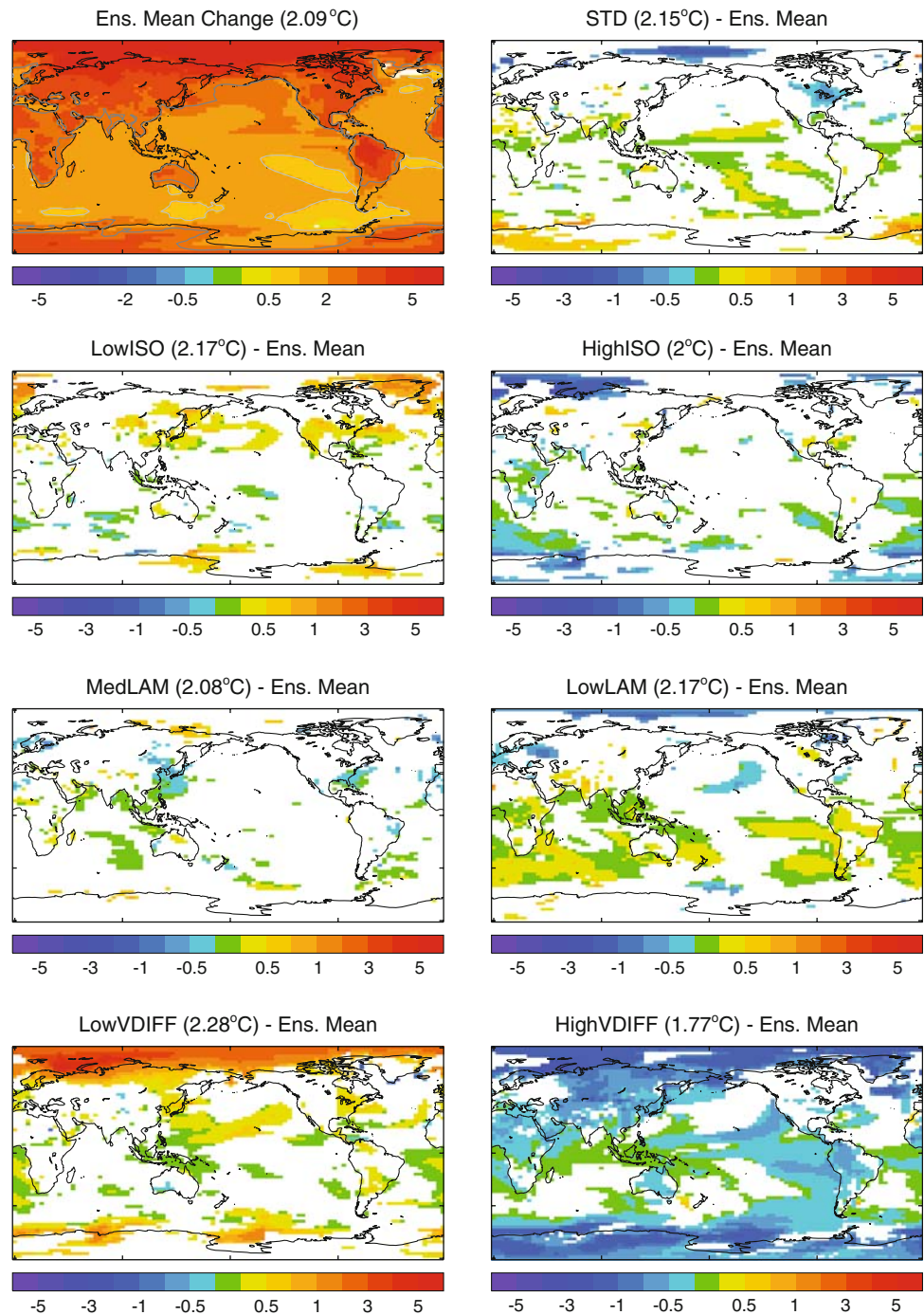
Fig. 8 The deviation in surface air temperature climate change signal of an ensemble member from the ensemble mean. The global mean surface air temperature change for each ensemble member is shown in the panel title. The values are only shown where they are significantly different from natural

is largest in the Arctic and around the coast of Antarctica, but there is also detectable spread throughout the tropics. Collins et al. (2006) created an ensemble to investigate the impacts of atmosphere parameter uncertainty on the climate response. They do not show a figure directly equivalent to Fig. 9, because the experimental set-up was slightly different. However, they do show the standard deviation of SAT in their ensemble (Collins et al. 2006, Fig. 10). As a simple rule of thumb, the 95% probability range is approximately ± 2 standard deviations for a normal distribution. This allows us to confirm that the atmosphere parameter uncertainty is more important than the ocean parameter uncertainty for the polar latitudes. The majority of the globe has a standard deviation less than their lowest level of 0.5°C. Figure 9 shows regions of the tropics that have an ocean parameter ensemble spread greater than 1°C.

An analysis of variations in the local radiative feedbacks (following e.g. Cess et al. 1990, Webb et al. 2006) was

Fig. 9 The ensemble range in the climate change signal. The range is only shown if it greater than that expected from natural variability

(a) Spread in SAT Change

0.25 0.75 1.5 3 5
Surface Air Temperature (K)

(b) Spread in Precip. Change

5 10 25 50 75 100 200
Precipitation (%)

(c) Spread in SST Change

0.25 0.75 1.5 3 5
Sea Surface Temperature (K)

(d) Spread in SSS Change
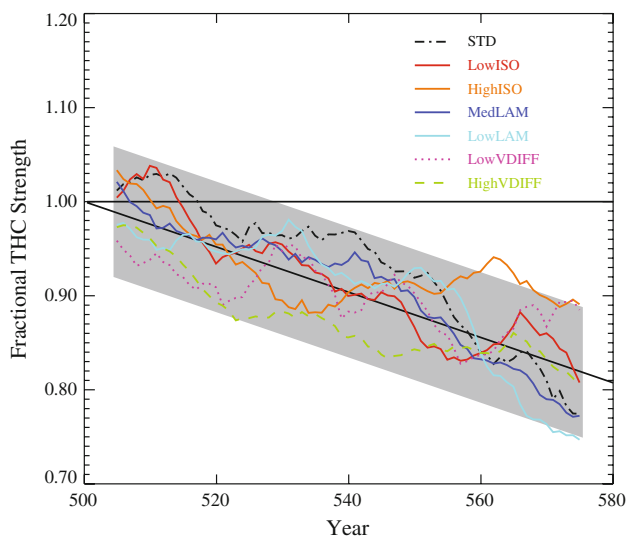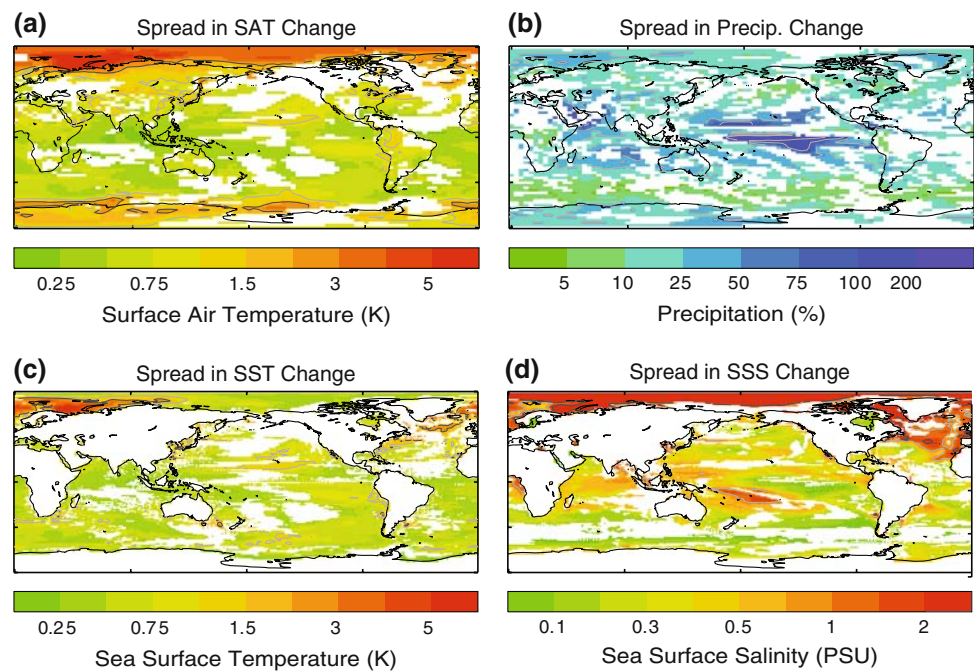
0.1 0.3 0.5 1 2
Sea Surface Salinity (PSU)

Fig. 10 The 10 year running-mean reduction in the meridional overturning circulation seen in each ensemble member. The strength is shown as fraction of the preindustrial THC strength. The *solid black line* shows the ensemble mean linear trend. The *grey shaded region* shows ±2 standard deviations of natural decadal variability calculated from a multi-millenia control simulation of HadCM3

performed to help explain the causes of some of the regional spread (figures omitted for brevity). It shows that the Arctic temperature spread is caused by uncertainty in the ice-albedo feedback, on top of a large mean signal. The large SAT spread in the eastern Pacific is co-located with the large spread in the baseline climate states—the feedback analysis shows that there is large uncertainty in the cloud radiative response in this region. The impact of

ocean-processes on the regional climate change pattern in the tropics are largely omitted (or highly simplified) in studies of cloud-feedbacks, as they concentrate on experiments in which either uniform SST changes are applied to atmosphere models or have simplified mixed-layer oceans. This study indicates that some representation of the impacts of perhaps rather subtle changes in tropical SSTs under climate change may be important.

Approximately 35% of the globe does not exhibit spread in the precipitation signal that is detectable above natural variability (this is uncoloured in Fig. 9). However, regions over the Southern Ocean and North Atlantic do show some detectable spread in precipitation response. Interestingly, these are the regions of the smallest mean surface temperature changes (Fig. 7). There is also detectable spread in each of the major equatorial convective regions: the maritime continent, West Africa and Amazonia. The largest percentage spread in the precipitation climate change signal is over the central Pacific, coincident with the differences in cloud radiative feedbacks discussed above.

5.4 The slowdown of the Atlantic meridional overturning circulation

The Atlantic meridional overturning circulation (MOC) has been the target of a large amount of research into the impact of parameters. Primarily this research has taken the form of sensitivity studies (e.g. Dalan et al. 2005a and Huang et al. 2003a), however there are a couple of perturbed parameter studies that investigate the change in the MOC strength, namely Collins et al. (2006), Hargreaves

et al. (2004) and Challenor et al. (2006). Table 2 shows that the mean MOC strength in the pre-industrial state varies across the ensemble, but within the range of other climate models. We find that only the perturbations to the vertical diffusivity cause statistically significant variations in the mean MOC strength in the baseline climate. However, the exact values do not fit the scaling laws of either Bryan (1987) or Dalan et al. (2005b). Huang et al. (2003a) find MOC sensitivity to the isopycnal diffusivity; however, this study can detect no link. The climate drifts in the deep ocean would impact the exact strength of the MOC, but will probably not impact the qualitative results.

There is large spread in the SSS climate change signal in the North Atlantic, therefore we may expect differences in the reduction of the MOC (no ensemble member has a complete shutdown). Figure 10 shows the 10-year running mean of the THC strength throughout the increasing CO_2 run, expressed as a fraction of each ensemble member's mean MOC strength in the control run. The ensemble mean linear trend is shown as the solid black line. The MOC has large decadal natural variability in each ensemble member (Table 1). The grey shaded area shows ±2 standard deviations of natural variability from the ensemble mean trend, which would be a 2.5–97.5% confidence interval if the variability were distributed normally. As none of the ensemble members fall substantially outside this shaded area it is not possible to determine whether the variations in the MOC reduction are caused by perturbations to ocean-model parameters or natural variability. Whether MOC reductions should be presented as absolute or fractional changes is an open question. It would be hard to prove a statistically significant ensemble spread even if absolute changes were used.

5.5 Summary of regional impacts assessment

C&07, and the analysis presented above, shows that perturbing certain ocean parameters in the HadCM3 model causes only relatively small impacts to global mean climate change. However, we do show here that there are spatial patterns of changes, associated with different perturbations, which are locally significant in some regions (i.e. greater than would be expected in the basis of natural variability). We conclude that the impact of uncertainties in ocean parameters should be considered when making probabilistic climate forecasts, especially for regions. The details of how this is done might, however, depend on the experimental design. Using the approach taken here, of spinning up each perturbed member until near-equilibrium, introduces surface climate biases which must be considered in any weighting scheme for producing probability distribution functions. An alternative approach (e.g. Murphy et al. 2007) would be

to use flux-adjustments to limit the development of surface biases. While weighting would be still be needed, the effect may be diminished when surface climates are constrained to be closer to observations. The spatial response might conceivably be also diminished with flux adjustments as the forced anomalies would be developing on similar baseline climate states.

6 Conclusions and discussion

This work describes an ensemble designed to investigate the possible impact of uncertainties in physical parameters in the ocean component of HadCM3 on simulations of climate change. Collins et al. (2007) presented the initial, global mean analysis of this ensemble. They found that the impacts of ocean parameter uncertainty on global mean climate response were relatively small. Firstly we have attempted to explain this result, and secondly we have investigated the potential impacts on the regional detail of the modelled climate change signal.

While the ocean heat uptake impacts of the parameter perturbations are in the expected directions, their magnitudes are generally small. They are also modified by interactions with other unperturbed ocean processes, which tend reduce the impacts further. These interactions require further study, but it is clear that understanding and modelling them are essential for predictions of ocean heat uptake. The ocean parameter perturbations cause detectable variations in regional climate change signals. Therefore a methodology that samples ocean parameter uncertainty is required when creating a probabilistic regional climate forecast, rather than creating a global-mean forecast. We also find that there is no detectable uncertainty in the meridional overturning circulation, partly because of its large natural variability.

The ensemble used for this investigation does not exhaustively sample all the uncertain ocean parameters in HadCM3. There are many other possible parameters that could be perturbed (see appendix) and these will be subject to future study. Structural uncertainty (relating to how the ocean model is created) was considered to be a large source of uncertainty by the majority of the experts consulted for this study. An experiment design to easily and systematically investigate structural uncertainty is not clear to the authors however. A substantial investment to design a flexible model platform would probably be required, although use of current ocean models and a flexible coupler such as the OASIS coupler (Valcke and Redler 2006) could provide a preliminary investigation. Incorporating additional ocean model uncertainties would, presumably, be expected to increase the spread in climate projections.

Appendix

Table 3

Table 3 Possible parameter perturbations for HadCM3 as determined by an expert consultation

Parameter (units)	Low	Medium	High	Switch options
Isopycnal diffusivity ($m^2 s^{-1}$)	200	**1,000**	2,000	
λ, δ in the mixed layer, (fraction, m)	0.3, 100	0.5, 50	**0.7**, 100	
Background vertical diffusivity ($10^{-5} m^2 s^{-1}$)	$0.5 - 4$	**1.0–15**	2–50	
Isopycnal viscosity ($m^2 s^{-1}$)	1,000	2,000	**3,000**	
Background thickness diffusivity	0	150	**350**	
Dependence of vertical viscosity on Richardson no. ($10^{-5} m^2 s^{-1}$)	3.0	**5.5**	8.0	
Background vertical viscosity ($10^{-5} m^2 s^{-1}$)	0.5	**1.0**	8.0	
Water type	II	**IB**	IA	
Visbeck coefficient ($m^2 s^{-1}$)	0.01	**0.015**	0.02	
K-Theory vertical mixing				**Pacanowski and Philander** (1981) or Peters et al. (1988)
Boundary layer scheme				**Quadratic** or quartic
Critical Richardson no. in boundary layer	0.25	0.3	**0.5**	
Maximum boundary layer depth	60	**80**	100	
Energy penetration from the mixed layer to below (fraction)	0.13	**0.15**	0.17	
Marginal Sea Outflow				Diffusive or **advective**
Haney Coefficient ($Wm^{-2} K^{-1}$)	81	**163**	572	

Three possible values are given for most parameters, however some of the perturbations are logical switches and their possible values are included in the final column

Bold type shows the standard HadCM3 value

References

Allan RJ, Ansell TJ (2006) A new globally complete monthly historical mean sea level pressure data set (HadSLP2): 1850–2004. J Clim 19(22):5816–5842. doi:10.1175/JCLI3937.1

Barkstrom BJ (1984) The earth radiation budget experiment (ERBE). Bull Am Meteorol Soc 65(11):1170–1185 10.1175/1520-0477(1984)065<1170:TERBE>2.0.CO;2

Barnett TP, Pierce DW, AchutaRao KM, Gleckler PJ, Santer BD, Gregory JM, Washington WM (2005) Penetration of human-induced warming into the world's oceans. Science 309(5732):284–287. doi:10.1126/science.1112418

Bryan F (1987) Parameter sensitivity of primitive equation ocean general circulation models. J Phys Oceanogr 17:970–985 10.1175/1520-0485(1987)017<0970:PSOPEO>2.0.CO;2

Bryden HL, Longworth HR, Cunningham SA (2005) Slowing of the Atlantic meridional overturning circulation at 25 N. Nature 438:655–657. doi:10.1038/nature04385

Cess RD, Potter GL, Blanchett JP, Boer GJ, DelGenio AD, Deque M, Dymnikov V, Galin V, Gates WL, Ghan SJ, Kiehl JT, Lacis AA, LeTruet H, Li ZX, Liang XZ, McAveney BJ, Meleshko VP, Mitchell JFB, Morcrette JJ, Randall DA, Rikus L, Roeckner E, Royer JF, Schlese U, Sheinin DA, Slingo A, Sokolov AP, Taylor KE, Washington WM, Wetherald RT, Yagai I, Zhang MH (1990) Intercomparison and interpretation of climate feedback processes in 19 atmospheric general-circulation models. J Of Geophys Research-Atmospheres 95(D10):16601–16615. doi:10.1029/JD095iD10p16601

Challenor PG, Hankin RKS, Marsh R (2006) Towards the probability of rapid climate change. In: Schellnhuber HJ, Cramer W, Nakicenovic N, Wigley T, Yohe G (eds) Avoiding dangerous climate change. Cambridge University Press, London, pp 55–63

Collins M, Booth B, Harris G, Murphy J, Sexton D, Webb M (2006) Towards quantifying uncertainty in transient climate change. Clim Dyn 27:127–147. doi:10.1007/s00382-006-0121-0

Collins M, Brierley CM, MacVean M, Booth BBB, Harris GR (2007) The sensitivity of the rate of transient climate change to ocean physics perturbations. J Clim 20(10):2315–2320. doi:10.1175/JCLI4116.1

Cubasch U, Meehl GA, Boer GJ, Stouffer RJ, Dix M, Noda A, Senior CA, Raper S, Yap KS (2001) climate change 2001: the scientific basis. Contribution of working group I to the third assessment report of the intergovernmental panel on climate change. In: Houghton JT, Ding Y, Griggs DJ, Noguer M, van der Linden PJ, Dai X, Maskell K, Johnson CA (eds) Projections of future climate change, vol Chap. 9. Cambridge University Press, London, pp 525–582

Cunningham SA, Alderson SG, King BA, Brandon MA (2003) Transport and variability of the Antarctic circumpolar current in

the drake passage. J Geophys Res 108(C5):8084. doi:10.1029/2001JC001147

Dalan F, Stone PH, Sokolov AP (2005a) Sensitivity of the ocean's climate to diapycnal diffusivity in an EMIC. Part II: global warming scenario. J Clim 18(13):2482–2496. doi:10.1175/JCLI3412.1

Dalan F, Stone PH, Kamenkovich IV, Scott JR (2005b) Sensitivity of the ocean's climate to diapycnal diffusivity in an EMIC. Part I: equilibrium state. J Clim 18(13):2460–2481. doi:10.1175/JCLI3411.1

Forest CE, Stone PH, Sokolov AP, Allen MR, Webster MD (2002) Quantifying uncertainties in climate system properties with the use of recent climate observations. Science 295(January):113–117. doi:10.1126/science.1064419

Gent PR, McWilliams JC (1990) Isopycnal Mixing in ocean circulation models. J Phys Oceanogr 20(January):150–155 10.1175/1520-0485(1990)020<0150:IMIOCM>2.0.CO;2

Gnanadesikan A, Slater RD, Swathi PS, Vallis GK (2005) The energetics of ocean heat transport. J Clim 18(14):2604–2616. doi:10.1175/JCLI3436.1

Gordon C, Cooper C, Senior CA, Banks H, Gregory JM, Johns TC, Mitchell JFB, Wood RA (2000) The simulation of SST, sea ice extents and ocean heat transports in a version of the Hadley Centre coupled model without flux adjustments. Clim Dyn 16:147–168. doi:10.1007/s003820050010

Gregory JM (2000) Vertical heat transports in the ocean and their effect on time-dependent climate change. Clim Dyn 16:501–515. doi:10.1007/s003820000059

Gregory JM, Mitchell JFB (1997) The climate response to CO_2 of the Hadley centre coupled AOGCM with and without flux adjustment. Geophys Res Lett 24(15):1943–1946

Gregory JM, Dixon KW, Stouffer RJ, Weaver AJ, Driesschaert E, Eby M, Fichefet T, Hasumi H, Hu A, Jungclaus JH, Kamenkovich IV, Levermann A, Montoya M, Murakami S, Nawrath S, Oka A, Sokolov AP, Thorpe RB (2005) A model intercomparison of changes in the Atlantic thermohaline circulation in response to increasing atmospheric CO^2 concentration. Geophys Res Lett 32(12). doi:10.1029/2005GL023209

Gregory JM, Lowe JA, Tett SFB (2006) Simulated Global-mean sea level changes over the last half-millennium. J Clim 19:4576–4591. doi:10.1175/JCLI3881.1

Hansen J, Ruedy R, Glascoe J, Sato M (1999) GISS analysis of surface temperature changes. J Geophys Res 104:30997–31022. Data available from http://data.giss.nasa.gov/gistemp/. doi:10.1029/1999JD900835

Hargreaves JC, Annan JD, Edwards NR, Marsh R (2004) An efficient climate forecasting method using an intermediate complexity Earth System Model and the ensemble Kalman filter. Clim Dyn 23(7–8):745–760. doi:10.1007/s00382-004-0471-4

Harris GR, Sexton DMH, Booth BBB, Collins M, Murphy JM, Webb MJ (2006) Frequency distributions of transient regional climate change from perturbed physics ensembles of general circulation model simulations. Clim Dyn 27:357–375. doi:10.1007/s00382-006-0142-8

Huang BY, Stone PH, Sokolov AP, Kamenkovich IV (2003a) Ocean heat uptake in transient climate change: Mechanisms and uncertainty due to subgrid-scale eddy mixing. J Clim 16(20):3344–3356 10.1175/1520-0442(2003)016<3344:OHUITC>2.0.CO;2

Huang BY, Stone PH, Hill C (2003b) Sensitivities of deep-ocean heat uptake and heat content to surface fluxes and subgrid-scale parameters in an ocean general circulation model with idealized geometry. J Of Geophys Research-Oceans 108(C1):3015. doi:10.1029/2001JC001218

Jones PD, New M, Parker DE, Martin S, Rigor IG (1999) Surface air temperature and its variations over the last 150 years. Rev Geophys 37:173–199. doi:10.1029/1999RG900002

Kraus EB, Turner JS (1967) A one-dimensional model of the seasonal thermocline II. the general theory and its consequences. Tellus 19(1):98–105

Legates DR, Willmott CJ (1990) Mean seasonal and spatial variability in global surface air-temperature. Theor Appl Climatol 41:11–21. doi:10.1007/BF00866198

Levitus S, Boyer T (1994) World Ocean Atlas. U.S. Department of Commerce, NOAA Atlas NESDIS, Washington, D.C

Marotzke J, Stone P (1995) Atmospheric transports, the thermohaline circulation, and flux adjustments in a simple coupled model. J Phys Oceanogr 25:1350–1364 10.1175/1520-0485(1995)025<1350:ATTTCA>2.0.CO;2

Meehl GA, Stocker TF, Collins WD, Friedlingstein P, Gaye AT, Gregory JM, Kitoh A, Knutti R, Murphy JM, Noda A, Raper SCB, Watterson IG, Weaver AJ, Zhao Z-C (2007) Climate change 2007: the physical science basis. Contribution of working group I to the fourth assessment report of the intergovernmental panel on climate change. Chap. Global Climate Projections. Cambridge University Press, Cambridge pp 747–845

Murphy JM, Sexton DMH, Barnett DN, Jones GS, Webb MJ, Collins M, Stainforth DA (2004) Quantification of modelling uncertainties in a large ensemble of climate change simulations. Nature 430:768–772. doi:10.1038/nature02771

Murphy JM, Booth BBB, Collins M, Harris GR, Sexton D, Webb M (2007) A methodology for probabilistic predictions of regional climate change from perturbed physics ensembles. Philos Trans R Soc A 365:1993–2028. doi:10.1098/rsta.2007.2077

Pacanowski RC, Philander SGH (1981) Parameterization of vertical mixing in numerical models of tropical oceans. J Phys Oceanogr 11:1443–1451

Peters H, Gregg MC, Toole JM (1988) On the parameterization of equatorial turbulence. J Geophys Res (Oceans) 93(C2):1199–1218

Randall DA, Wood RA, Bony S, Colman R, Fichefet T, Fyfe J, Kattsov V, Pitman A, Shukla J, Srinivasan J, Stouffer RJ, Sumi A, Taylor KE (2007) Climate Change 2007: The Physical Science Basis. Contribution of Working Group I to the Fourth Assessment Report of the Intergovernmental Panel on Climate Change. Chap. Climate Models and Their Evaluation. Cambridge University Press, Cambridge pp 589–662

Rayner NA, DE Parker , Horton EB, Folland CK, Alexander LV, Rowell DP, Kent EC, Kaplan A (2003) Global analyses of sea surface temperature, sea ice, and night marine air temperature since the late nineteenth century. J Geophys Res 108(D14):4407. doi:10.1029/2002JD002670

Russell JL, Stouffer RJ, Dixon KW (2006) Intercomparison of the Southern Ocean circulation in IPCC coupled model control simulations. J Clim 19(18):4560–4575. doi:10.1175/JCLI3869.1

Schmitz WJ (1996) On the World Ocean circulation: volume I. Some global features/North Atlantic circulation. Technical Report WHOI-96-03. Woods Hole Oceangraphic Institution

Stainforth DA, Aina T, Christensen C, Collins M, Frame DJ, Kettleborough JA, Knight S, Martin A, Murphy J, Piani C, Sexton D, Smith LA, Spicer RA, Thorpe AJ, Webb MJ, Allen MR (2005) Uncertainty in predictions of the climate response to rising levels of greenhouse gases. Nature 433(7024):403–406. doi:10.1038/nature03301

Stouffer RJ, Manabe S (2003) Equilibrium response of thermohaline circulation to large changes in atmospheric CO_2 concentration. Clim Dyn 20(7):759–773. doi:10.1007/s00382-002-0302-4

Taylor KE (2001) Summarizing multiple aspects of model performance in a single diagram. J Geophys Res 106(D7):7183–7192. doi:10.1029/2000JD900719

Top500 org (2004) http://www.top500.org/list/2004/11/100

Valcke S, Redler R (2006) OASIS4 user guide. Tech Rep TR/CMGC/00-10. CERFACS

Webb MJ, Senior CA, Sexton DMH, Ingram WJ, Williams KD, Ringer MA, McAvaney BJ, Colman R, Soden BJ, Gudgel R, Knutson T, Emori S, Ogura T, Tsushima Y, Li B, Androva N, Musat I, Bony S, Taylor KE (2006) On the contribution of local feedback mechanisms to the range of climate sensitivity in GCM ensembles. Clim Dyn 27:17–38. doi:10.1007/s00382-006-0111-2

Whitworth T, Petersen RG (1985) Volume transport of the Antarctic circumpolar current from bottom pressure measurements. J Phys Oceanogr 15:810–816 10.1175/1520-0485(1985)015<0810:VTOTAC>2.0.CO;2

Wigley TML, Raper SCB (2001) Interpretation of high projections for global-mean warming. Science 293(5529):451–454. doi:10.1126/science.1061604

Xie P, Arkin PA (1996) Analyses of global monthly precipitation using gauge observations, satellite estimates, and numerical model predictions. J Clim 9:840–858 10.1175/1520-0442(1996)009<0840:AOGMPU>2.0.CO;2